frontiers | Frontiers in Earth Science

TYPE Original Research
PUBLISHED 19 June 2024
DOI 10.3389/feart.2024.1412827

OPEN ACCESS

EDITED BY
Paolo Capuano,
University of Salerno, Italy

REVIEWED BY
Umberto Tammaro,
National Institute of Geophysics and Volcanology (INGV), Italy
Simona Petrosino,
Istituto Nazionale di Geofisica e Vulcanologia, Italy

*CORRESPONDENCE
Monika Przeor,
monikaprzeor@hotmail.com

RECEIVED 05 April 2024
ACCEPTED 28 May 2024
PUBLISHED 19 June 2024

CITATION
Przeor M, D'Auria L, Pepe S, Tizzani P, Barone A, Vitale A, Pérez NM and Castaldo R (2024), Independent component analysis and finite element modelling of the 2004–2005 ground deformation in Tenerife (Canary Islands).
Front. Earth Sci. 12:1412827.
doi: 10.3389/feart.2024.1412827

Independent component analysis and finite element modelling of the 2004–2005 ground deformation in Tenerife (Canary Islands)

Monika Przeor[1,2]*, Luca D'Auria[1,2], Susi Pepe[3], Pietro Tizzani[3], Andrea Barone[3], Andrea Vitale[3], Nemesio M. Pérez[1,2] and Raffaele Castaldo[3]

[1]Instituto Tecnológico y de Energías Renovables, Santa Cruz de Tenerife, Spain, [2]Instituto Volcanológico de Canarias (Involcan), Puerto de la Cruz, Spain, [3]Istituto per il Rilevamento Elettromagnetico dell'Ambiente (IREA-CNR), Napoli, Italy

Historic volcanic activity in Tenerife was concentrated within two of the island's three dorsals and on the Teide-Pico Viejo complex located inside Las Cañadas caldera. Eruptions on the island are primarily characterised by basaltic and trachybasaltic fissural eruptions. However, the Teide-Pico Viejo complex also hosted explosive and effusive phonolitic eruptions. Our study focused on the analysis of the 2004–2005 unrest in Tenerife, which was characterised by an onset of a ground deformation pattern, heightened on-land seismic activity, changes in the chemical composition of fumaroles of the Teide composite volcano, an increase in diffusive emissions of carbon dioxide along the NW rift, and, significant gravity changes. We used the Envisat-ASAR satellite images from 2003 to 2010 to generate the Line-Of-Sight SBAS-DInSAR deformation time series to investigate the source responsible for ground deformation. We applied the Independent Component Analysis (ICA) to separate distinct ground deformation patterns. Specifically, we selected four components for the Independent Component Analysis decomposition: the first one mainly affects the stratovolcano's summit region of Teide and shows a circular symmetry; the second and third components are possibly related to the topography and atmospheric artifacts, while the fourth contains only a noisy signal. We employed a non-linear optimisation approach in a Finite Element modelling environment to determine the source geometry responsible for the first identified ICA pattern of ground deformation within Las Cañadas. Our results revealed the existence of an ellipsoidal ground deformation source oriented along the E-W axis, located beneath the Teide and Montaña Blanca volcanoes at 1,600 m a.s.l. This source became active during the seismic crisis of 2004–2005, which was associated with the degassing of a magma batch that intruded into the northwest rift of Tenerife island. We propose that the ground deformation observed at Teide volcano during the 2004–2005 crisis was related to hydrothermal activity within the volcano.

KEYWORDS

DInSAR SBAS, volcano geodesy, finite element modeling (FEM), independent component analysis (ICA), Tenerife, Canary Islands

1 Introduction

Tenerife is the largest island in the Canaries. Due to its high population density and five historical eruptions in the last five centuries, it is considered a region with a moderate volcanic risk (Carracedo et al., 2007). The island's formation began as a Shield Volcanic Complex (SVC) in the Miocene period, possibly consisting of three independent islands: Anaga, Teno, and Roque del Conde massifs (Barrera Morate and García Moral, 2011). Its structural evolution was completed during the Pliocene, followed by a stage of formation of the central part of the island known as the Las Cañadas edifice. This building phase merged the previous shield volcanoes into a single island. During the Pleistocene, the ongoing formation of Las Cañadas caldera was also marked by numerous strombolian eruptions with vents located along the rifts (NE-SW, N-S and NW-SE) connecting Las Cañadas and the older shield volcanoes. The rapid development of Las Cañadas was later followed by destructive episodes characterised by massive lateral collapses, leading to the formation of the current Las Cañadas Caldera (Barrera Morate and García Moral, 2011). Strombolian activity in the rifts remained prominent, and Las Cañadas Caldera was filled with salic eruptions, creating the Teide-Pico Viejo complex and peripheral eruptions within the Las Cañadas domain. The Holocene activity was concentrated on eruptions occurring in the island's rifts but also affecting the Las Cañadas domain. From the 16th century to the present, five historical eruptions were concentrated mainly on the NW-SE and NE-SW dorsals, with only one occurring on the Teide-Pico Viejo complex. However, even though historical eruptions displayed basaltic fissure volcanic activity, Teide-Pico Viejo's activity included effusive and explosive eruptions of phonolitic magmas. The most recent explosive eruption in Tenerife was the sub-Plinian eruption of Montaña Blanca, which occurred approximately 2000 years ago (Figure 1) (Barrera Morate and García Moral, 2011). The most recent eruption of the Teide stratovolcano complex occurred roughly 800 years ago and is evident in the phonolitic lava flows that descend from the summit cone (Barrera Morate and García Moral, 2011). Currently, the Teide stratovolcano is dormant; its background volcanic activity consists mainly of a continuous microseismicity of Volcano-Tectonic (VT) and Long-Period (LP) events, fumarole activity in the crater of Teide and diffuse degassing (Koulakov et al., 2023).

At the beginning of 2001, anomalous seismic activity on the island began, with higher-than-background seismicity values registered by Instituto Geográfico Nacional (IGN) (Gottsmann et al., 2006; Almendros et al., 2007; Martí et al., 2009) and geochemical anomalies (Weber et al., 2006; Melián et al., 2012; Pérez et al., 2013). The most critical episode that prompted a "volcanic unrest alert" to be issued to the local government was the intense seismic activity that started in April 2004 and persisted until July 2005 (Almendros et al., 2007; Martí et al., 2009; Pérez et al., 2013). This seismicity was characterised by volcano-tectonic events located within the Las Cañadas domain and some long-period events (Almendros et al., 2007).

During this period of seismic unrest, the chemical composition of gases in Teide fumaroles indicated the presence of magmatic SO_2, and there was also an increase in diffuse CO_2 emissions in the northwest rift zone (Pérez et al., 2013). Furthermore, in the local galleries within the southern rift of the island, it was observed an increase in radon emission (^{220}Rn and ^{222}Rn) and an increase in the SO_2/Cl ratio in the groundwater (Melián et al., 2012). Gottsmann et al. (2006) evidenced a gravity increase in the northern flank of the Teide-Pico Viejo volcanic complex and a lack of significant ground deformation. However, Fernández et al. (2009) identified evidence of ground deformation of just a few centimeters in the Teide-Pico Viejo volcanic complex in 2004. At the same time, these authors also identified continuous subsidence in Las Cañadas triggered by the compressional state of the volcanic edifice (Fernández et al., 2009). The intense seismic activity persisted until July 2005 and gradually decreased throughout the early months of the following year (Almendros et al., 2007). The observed volcanic crisis did not culminate in an eruption, and, as mentioned by Melián et al. (2012), the possibility of the reactivation of the Teide-Pico Viejo was low.

Even though a ground deformation in 2004 was observed (Fernández et al., 2009), until now, no modelling of the causative source has been presented. We believe that a better understanding of this episode would allow a better understanding of the dynamics of the volcanic hydrothermal system of Tenerife and, consequently, would provide a useful tool for the interpretation of future volcanic unrest episodes on the island.

We first performed data processing employing the Differential Interferogram Satellite Aperture Radar (DInSAR) by using the Small BAseline Subset (SBAS) algorithm (Figure 2). Then we applied the Independent Component Analysis (ICA) to the 2004–2005 ground deformation occurring in Tenerife, obtaining the decomposition of the signal in different components. Applying the ICA to this dataset allowed us to identify a consistent ground deformation pattern that we attributed to a causative volcanic source. We modelled this pattern using a non-linear optimisation within a Finite Element (FE) environment to study the geometry of the source in detail.

Interferogram stacking (DInSAR SBAS) is a widely known method for processing the SAR data in order to obtain time series of cumulative deformation in the area of interest. In this method, the multiple interferograms with the Small Baseline between the SAR images are overlaid, allowing to obtain small displacement information along the long time periods. The DInSAR SBAS method was proposed by Bernandino et al. (2002) using the SAR images acquisitions with a small orbital separation (SBAS), allowing limiting the observed spatial decorrelation phenomena. This method was widely applied to study volcanic behaviours (Tizzani et al., 2007; Pepe et al., 2008; De Luca et al., 2015; Pepe et al., 2018) where prolonged deformation in time within the volcanic areas was observed.

The Independent Component Analysis (ICA) represents a valuable statistical tool for analysing complex datasets (Comon, 1994; Hyvärinen and Oja, 2000). It allows the decomposition of a mixture of signals under the assumption that the individual sources are statistically independent and non-Gaussian (Ebmeier, 2016). ICA enables the separation of a dataset into non-orthogonal components that exhibit minimal statistical dependence between them. This valuable technique was first introduced for computational signal processing. However, it has also been applied in various geophysical applications like volcano seismology (Acernese et al., 2004) and volcano geodesy (Bottiglieri et al., 2007; Ebmeier, 2016; Przeor et al., 2022).

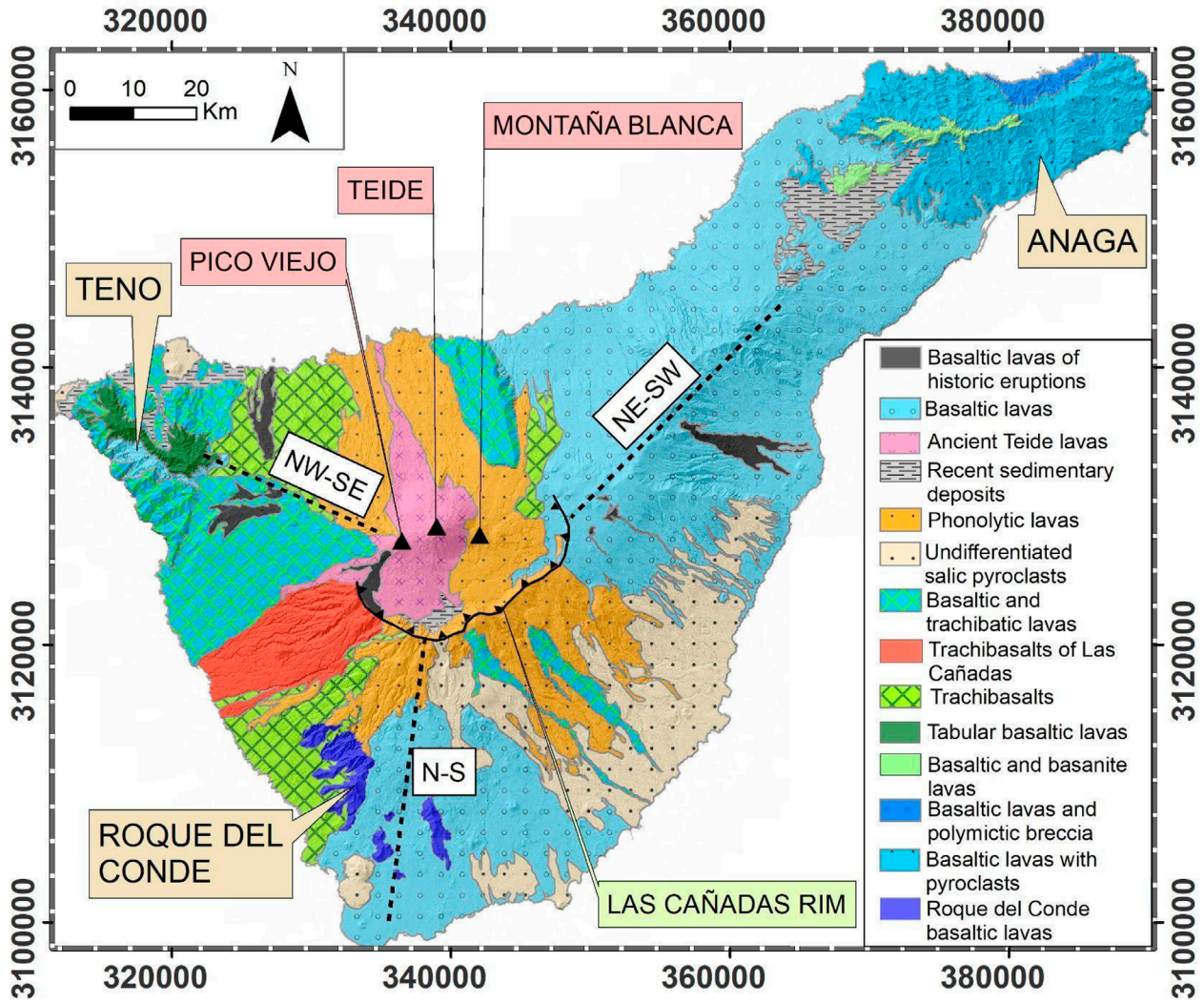

FIGURE 1
Geological map of Tenerife after Barrera Morate and García Moral (2011). The legend explains the meaning of the color shades on the map. The three SVCs are marked with the tanned yellow square with the SVCs' names included. The rim of the caldera is shown with black lines and triangles. Black triangles represent the volcanoes Pico Viejo, Teide, and Montaña Blanca. A dashed black line represents the three rifts.

The ICA in the volcano geodesy context has been applied to GNSS and DInSAR datasets and has shown its effectiveness in reducing the noise and uncovering hidden ground deformation patterns within complex DInSAR datasets. Ebmeier (2016) showcased its effectiveness in separating the causative sources of complex ground deformation. Subsequently, Przeor et al. (2022) used ICA to separate independent components of ground deformation in Hawaii, highlighting its ability to identify simultaneous but independent sources acting beneath Mauna Loa and Kīlauea volcanoes.

The observed ground deformation was modeled within the Finite Element environment in order to modelise the geometry and the location of the source responsible for the observed anomalies. This method is commonly applied to the DInSAR dataset, which helps visualizing the magmatic or hydrothermal sources. The application of this method to the DInSAR SABS dataset of Sentinel-1 allowed modelise the magmatic source injection during the pre-eruptive episode in La Palma (Tajogaite eruption of 2021); (De Luca et al., 2022).

2 Methodology

2.1 SBAS DInSAR time series

The data used in this study were collected by the European Space Agency (ESA) through the ASAR sensor onboard the Envisat satellite acquired on C-band wavelength (≈5.6 cm). The satellite images acquired along ascending orbits were analyzed by the Grid Processing On Demand (G-POD) platform of ESA applying the multitemporal analysis using the Small BAseline Subset (SBAS) to obtain the Line-Of-Sight (LOS) time series for the coherent pixels of the SAR dataset (De Luca et al., 2015). The obtained 180 interferograms were processed with a maximum temporal

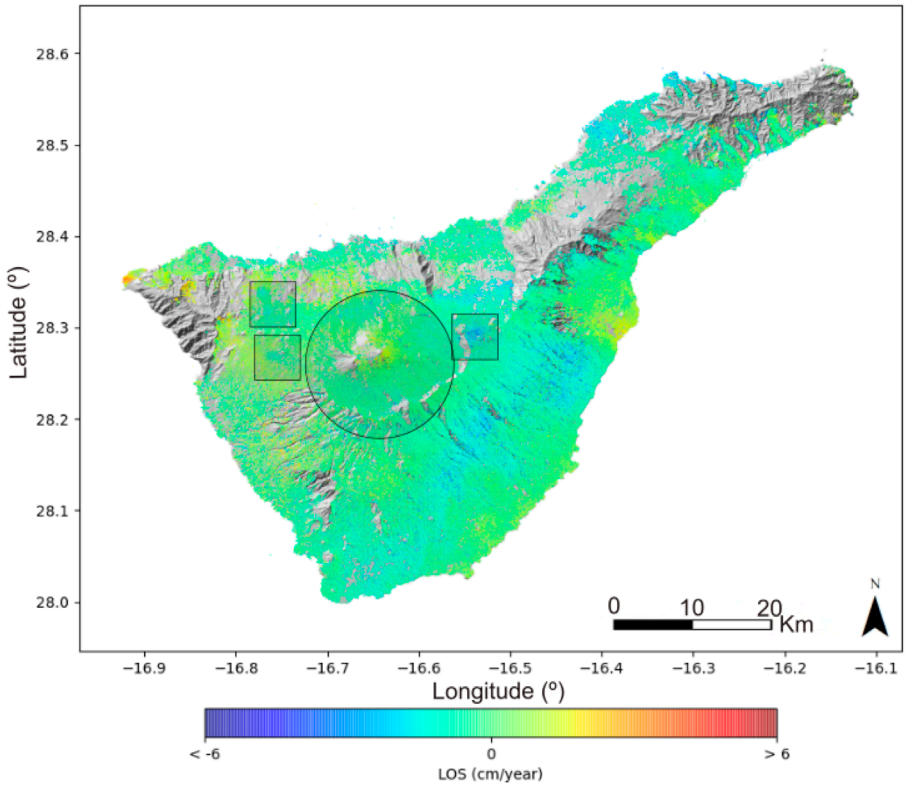

FIGURE 2
The 2003–2005 SBAS-DInSAR mean velocity map represented in Line-Of-Sight (cm/year). The black circle shows the area of interest where the ICA decomposition is applied. In contrast, the three black squares represent the zones of the local negative deformation, discussed by Fernández et al. (2009).

baseline of 150 days and a maximum spatial baseline of 400 m. We achieved the time series for each coherent pixel for the ascending orbit encompassing the island of Tenerife between 2003 and 2010. However, since the ground deformation occurred between 2004 and 2005, we focused on the dataset encompassing this interval. We did not evidence of any ground deformation pattern in the subsequent period in the processed dataset.

2.2 Independent component analysis (ICA) of SBAS DInSAR time series

In the context of an SBAS DInSAR dataset, the time series is represented as L (x_i, t_j), where L denotes the Line-Of-Sight (LOS) displacement, x_i corresponds to the position of the ith DInSAR pixel, and t_j represents the time of the jth DInSAR image (see Eq. 1). The DInSAR dataset can be decomposed into a finite sum of N components characterised by fixed spatial patterns. If we denote B_k *the* spatial pattern of the kth and with A_{jk} *the* time-varying amplitudes of the kth component in time t_j, we can write the ICA decomposition result as:

$$L(x_i, t_j) = \sum_{k=1}^{N} A_{jk} B_k(x_i) \quad (1)$$

Once the spatial patterns have been normalised, the sum of squared amplitudes A_{jk} for each independent component k defines its energy. This enables us to sort the components based on their energy and determine the optimal number of components representing the whole signal. This can be realised by setting a threshold below which the contribution to the total energy is negligible. We opted to retain one more component, even if characterised by negligible amplitude values, given that it would host the noise inherent in each DInSAR dataset. In the case of the ascending SBAS DInSAR dataset for Tenerife, we used four components.

2.3 Non-linear source modeling through the finite element modeling

To model a causative source of ground deformation, represented by an individual ICA component, we employed the Comsol Multiphysics® software environment. We built a three-dimensional mesh taking into account Tenerife Island's topography. The computational domain had dimensions of 33,000 m along the EW direction, 25,000 m along the NS direction, and 12,000 m in depth, to cover all the Las Cañadas caldera. We assumed isotropic linear elastic material properties. The elastic constants are calculated assuming an average P-wave velocity of 4,000 m/s, S-wave velocity of 2,400 m/s, and a 2,700 kg/m^3 density. The seismic wave velocity values have been estimated from the seismic tomography model of Koulakov et al. (2023).

The domain was discretised using tetrahedral mesh elements, with a maximum element size of 1,200 m and a minimum element size of 500 m. As a starting model, we chose a three-axis body representing the causative sources of the observed ground deformation. The parameters used to define the source model are seven: the center position in UTM (X, Y, Z); the dimensions of the ellipsoid axes along the X, Y, and *Z*-axes in meters; and the overpressure in pascals (Pa). The best-fit model has been retrieved through a non-linear optimisation using the Nelder and Mead (1965) simplex algorithm. The number of iterations required to reach the minimum was 1,000, and an objective function used was the residual sum of squares.

3 Results

3.1 SBAS DInSAR time series

The 2003–2005 SBAS DInSAR mean LOS velocity map computed along ascending orbit reveals four local deformation patterns on the island (Figure 2). At first sight, three areas of deformation with negative values are visible, one located in the NE-SW rift and two in the NW-SE rift, highlighted by black squares in Figure 2. These ground deformation anomalies were previously identified by Fernández et al. (2009) and associated with water withdrawal from the island's galleries. As this study aims to identify ground deformation caused by volcanic or hydrothermal activity, we chose not to focus on these hydric ground deformation behaviours. The central area of Tenerife, in the Teide volcano, exhibits a positive ascending LOS deformation of a few cm/year. The deformation encompasses all of the Teide volcano area; however, the deformation is interspersed with other patterns visible on the DInSAR dataset. The application of ICA helped us to understand the geometry and more precise location of the area affected by the ground deformation at Teide. To better analyze the ICA patterns, we selected a radius of 9 km from the summit cone of Teide, shown by the black circle in Figure 2.

3.2 Application of the ICA to the DInSAR dataset

The results of ICA decomposition to the SBAS DInSAR dataset within the area of 9 km of radius from the summit of the Teide volcano revealed the presence of at least four components (Figure 3), sorted in descending order by their energy. Among these, three exhibited significant ground deformation values, while the fourth component had low amplitude energy and primarily consisted of noise. The first component of the ICA decomposition (ICA1) exhibits a highly localized and high-energy pattern, with the maximum within the summit cone of the Teide volcano (see panel A in Figure 3), displaying a circular symmetry with an approximate radius of 3 km.

The second and third components of the ICA decomposition (ICA2 and ICA3; panels B and C of Figure 3) likely represent topographical or atmospheric artifacts with high ICA energy values (Table 1). The ICA2 represents the negative values on the northern flank of the complex volcano and higher positive values on the southern side of the Teide. The positive values are located exactly in the edge of the Las Cañadas rim while the negative ones are located in the northern side of the flank of Teide. The topography in Tenerife is abrupt and presents very complex features. The SBAS method cannot eliminate the whole signal corresponding to the topography, however, by applying the ICA we can discard the left pattern of topography from the data. The ICA3 is less energetic and does not have locally concentrated anomalies. However, as the SBAS method can still allow having the atmospheric artifacts in the dataset, we associate this pattern with the atmospheric noise. The final component (ICA4; panel D of Figure 3) displays a negligible signal pattern and possesses low energy (Table 1), indicating that it primarily represents signal noise.

3.3 Non-linear optimization in finite element modeling

The inverse modeling was carried out on the first component of the ICA (ICA1) due to 1) its high ICA energy, 2) the location in the area of the highest interest, and 3) the potential volcanic or hydrothermal origin of deformation. In the following, we provide details of the optimization results (see Table 2 for optimisation parameters). The results of the inverse modeling, as indicated by the local maximum in the Teide summit cone, exhibit a substantial adjustment with the observed data (Figure 4). The parameters defining the source responsible for the observed deformation were determined based on an ellipsoidal geometry positioned at 1,600 m a.s.l. This source is situated beneath the summit zone of the Teide volcano, with dimensions of 1,420 m, 893 m, and 536 m along the X, Y, and *Z*-axes, respectively. The location of the source in UTM was the following: X= 340075 mE; Y= 3128959 mN (UTM zone 28R) (see Table 2). The geometry of this source demonstrated nearly perfect alignment with the ICA1 data, resulting in low residuals (Figure 4C).

4 Discussion and conclusion

The detected ground deformation in Tenerife was analyzed by applying ICA to the DInSAR dataset, which was achieved by data processing of the ascending Envisat satellite images. The main volcanic deformation source in Tenerife was identified in the first ICA component, primarily concentrated between 2004 and 2005. The geometry of the source was derived through inverse modeling, assuming a three-axial ellipsoidal source located beneath the Teide and Montaña Blanca volcanoes at 1,600 m a.s.l. (Figure 5). Our results show a deformation source elongated mainly along the E-W axis. The current study findings strongly suggest that a ground deformation source was activated during the seismic crisis in 2004–2005. These results are compatible with the conclusions of previous studies, where a volcanic or hydrothermal origin in the Teide volcano was distinctly established through various geophysical and geochemical methods (García et al., 2006; Gottsmann et al., 2006; Tárraga et al., 2006; Weber et al., 2006; Almendros et al., 2007; Carracedo et al., 2007; Gottsmann et al., 2008; Márquez et al., 2008; Fernández et al., 2009; Martí et al., 2009; Domínguez-Cerdeña et al., 2011; De Barros et al., 2012; Melián et al., 2012; Pérez et al., 2013). In the following, we

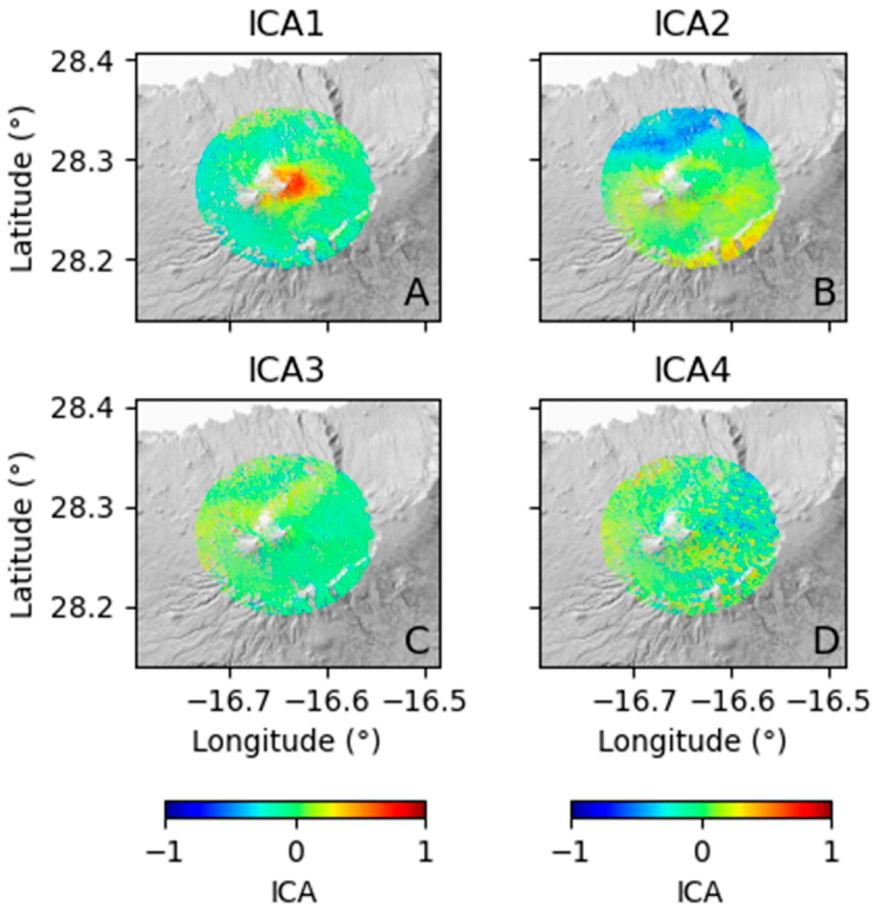

FIGURE 3
Four independent component maps **(A–D)** extracted by ICA within the selected area of a 9 km radius from the summit of the Teide volcano. The amplitude of the ground deformation pattern components is normalized.

TABLE 1 ICA components and their respective energy.

Component	Energy (%)
ICA1	32.4
ICA2	31.9
ICA3	24.7
ICA4	11.0

TABLE 2 Optimized source parameters.

X (UTM)	Y (UTM)	Depth (m)	Rx (m)	Ry (m)	Rz (m)
340078	3128959	−1,603	1,421.6	893.5	536

describe the similarities and differences observed between the previous studies and the present one.

The most significant feature during the crisis of 2004–2005 was primarily focused on seismic activity in the area of the Teide volcano and the NW rift of the island (Tárraga et al., 2006; Almendros et al., 2007). Tárraga et al. (2006) postulated the existence of volcanic tremor caused by convective processes in the reservoir beneath the Teide-Pico Viejo volcanic complex triggered by new inputs of magma. However, according to Almendros et al. (2007), the 2004–2005 crisis was marked by anomalous seismic events triggered by deep magma injection under the NW flank of Teide. This new input of magma triggered the VT earthquakes, the release of magmatic gases, and, consequently, LP events. Ultimately, the injection of magma into the crust disturbed the local aquifers in Las Cañadas and induced volcanic tremor beneath the Teide volcano. Both authors confirm the evidence of the magmatic reactivation of the Teide volcano.

Additionally, Gottsmann et al. (2006), through joint microgravity and ground deformation surveys realized in May 2004 and July 2005, observed changes in the gravity field but found no evidence of significant ground deformation caused by volcanic phenomena. They could not detect these slight changes in ground deformation due to the lack of a network covering the area of interest and the temporary nature of the stations. However, applying the Envisat ASAR dataset that covers all the areas of interest and samples the data every 35 days during the 9 years of analysed

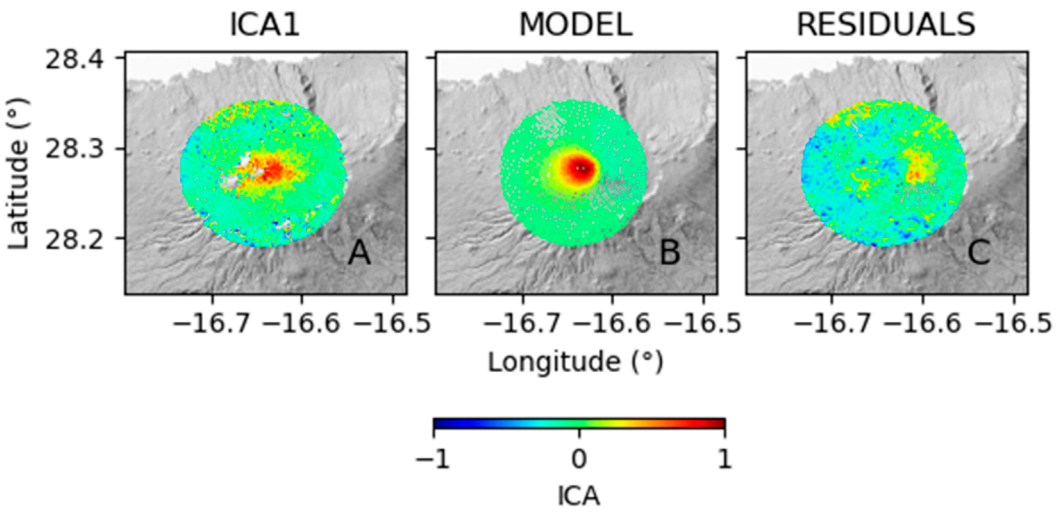

FIGURE 4
Modelling result **(A)** data, **(B)** model, and **(C)** residuals for the inverse modeling of the first component of the ICA decomposition, respectively. The amplitude of the ground deformation pattern components is normalized.

period, we were able to detect even small changes in the ground deformation behavior. In addition, the ICA method decomposes the raw DInSAR SBAS signal into independent signal behaviours, letting the small changes in the ground deformation be noticed.

Gottsmann et al. (2006) proposed three possible scenarios for the observed gravity increase: 1) new magma inputs, 2) migration of hydrothermal fluids, or 3) a hybrid process involving both a new magma input and hydrothermal fluid migration. To support the hypothesis of hydrothermal fluid migration, the authors conducted an inversion of the gravity data and determined that a hydrothermal reservoir was responsible for the observed changes. Their results indicate the existence of the source at a depth of 1,9 +- 0.12 km below the surface, which is approximately consistent with our results showing the source at a depth of 1,600 m a.s.l. Ultimately, Gottsmann et al. (2006) concluded that the movement of hydrothermal fluids is the most likely scenario to explain the gravity changes and the absence of ground deformation. However, the present study allowed us to uncover hidden deformation patterns in the Teide volcano, providing further insight into the dynamics of the 2004–2005 unrest.

Additionally, Martí et al. (2009) evaluated seismic and microgravimetric observations, finding clear evidence of volcanic activity on the Teide volcano. Their discussion was based on the number and location of VT and LP events, tremor, and perturbations in the gravity field. They also reported increased activity in the fumaroles of Teide and the appearance of new fractures with gas emissions in La Orotava. These anomalies were interpreted as disturbances in the background activity of the Teide-Pico Viejo volcanic complex. The authors postulate that new magma inputs can trigger the reactivation of the phonolitic reservoir beneath the Teide-Pico Viejo volcanic complex in the future.

Furthermore, Fernández et al. (2009) identified three distinct areas affected by ground deformation in Tenerife using DInSAR SBAS data from the ERS-1 and ERS-2 sensors between 1995 and 2005. The primary one was characterized as the compressional state of the island, attributed to the gravitational load of the edifice. Additionally, there were very localized subsidence zones in the rifts of the island, which were attributed to water withdrawal in the galleries, evidenced by Fernández et al. (2009) and also shown in Figure 2 in the present study. The authors also observed disturbances in ground deformation in the Teide volcano associated with the volcanic crisis; however, they did not perform modeling of the causative source for the observed ground deformation between 2004 and 2005.

Finally, through the geochemical analysis, Melián et al. (2012) observed a change in the composition of fumaroles in the Teide crater, resulting in a higher contribution of magmatic gases between 2001 and 2005. Pérez et al. (2013) reported temporal changes in the gas composition of Teide's fumaroles, including increased CO_2 efflux in the Teide summit cone and crater since 2001. They highlighted that the Teide volcanic and hydrothermal system undergoes temporal degassing episodes caused by magmatic fluid injection into the hydrothermal system, which was evident in 2004 and triggered by magma movements beneath Teide. Additionally, they rejected the previously proposed hypothesis by Martí et al. (2009) regarding the reactivation of the phonolitic storage of Teide-Pico Viejo due to the analysis of gas compositions in fumaroles by Melián et al. (2012) and SO_2 emissions reported by Weber et al. (2006).

The reactivation of an ellipsoidal-like source beneath the Teide volcano offers a comprehensive understanding of the seismic, gravimetric, and geochemical anomalies that occurred during the 2004–2005 crisis.

First of all, we observe that the ground deformation source we identified is located at a shallower depth and is displaced about 5 km to the SE with respect to the northern seismic cluster active during 2004 (Domínguez-Cerdeña et al., 2011). This seismic cluster has been interpreted by different authors as the effect of a magmatic intrusion in the north-western part of Tenerife (Gottsmann et al., 2006; Domínguez-Cerdeña et al., 2011). The volume affected by

10.3389/feart.2024.1412827

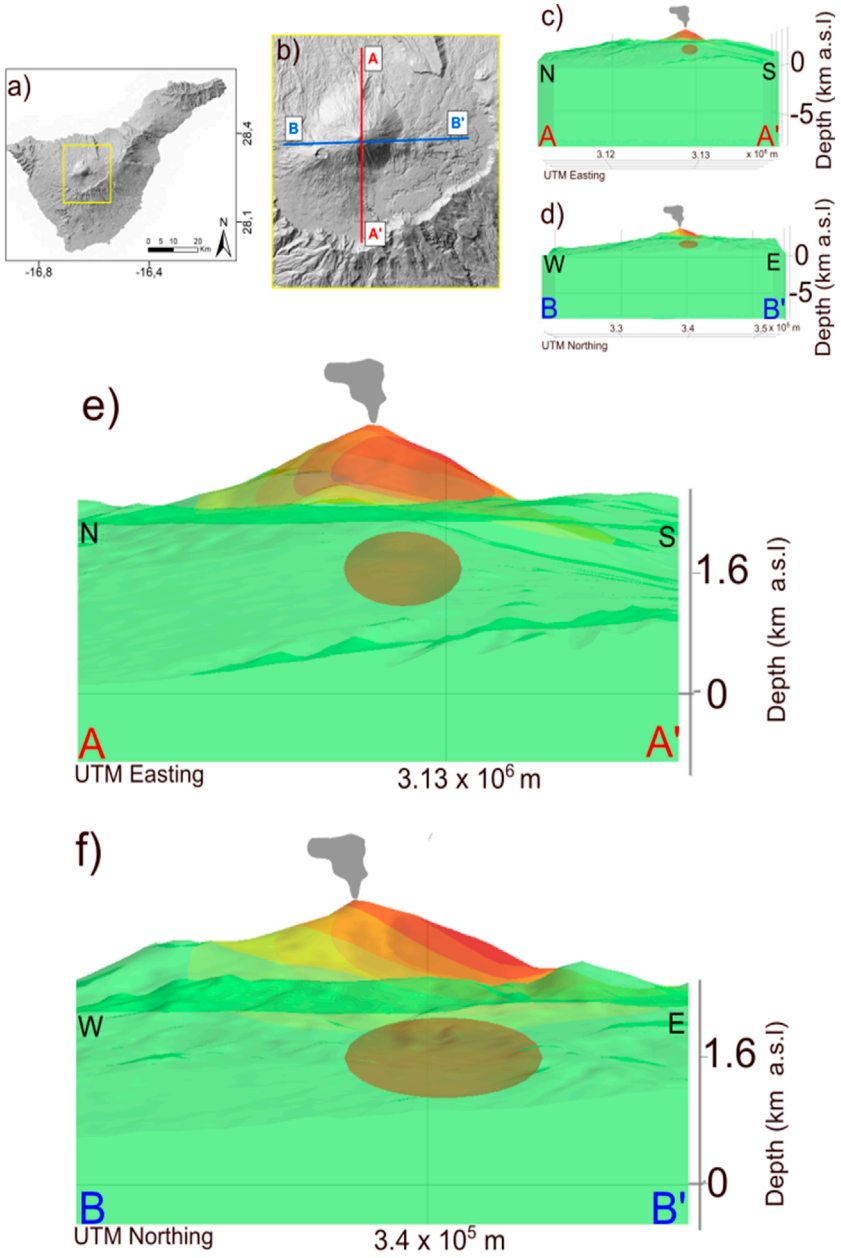

FIGURE 5
Three-dimensional model of the retrieved source responsible for the 2004–2005 ground deformation. **(A)** Map of Tenerife island, with the yellow box indicating the zoom of the Las Cañadas region. **(B)** Las Cañadas region, featuring the N-S **(A,A′)** and E-W **(B,B′)** profiles, is employed to represent the vertical sections of topography and the source **(C,D)** The N-S and E-W sections of the topography in Las Cañadas and the ground deformation modeled source, while **(E,F)** shows the enlarged views of panels **(C,D)**.

this cluster has shown limited activity in the following years (Koulakov et al., 2023).

Secondly, Gottsmann et al. (2006) evidenced that the observed gravity variations are compatible with a density increase caused by the filling of rock porosity with hydrothermal fluids. They assume a volume fraction of 30% and infer a source having a radius of around 80 m. Assuming a larger source volume, the volume fraction decreases. Our source model has a volume of approximately 2.8×10^9 m^3, which implies a much lower volume fraction. Another possibility is that the source thickness would be much lower than its areal extension or, in other words, it consists of a sill-shaped geometry. Unfortunately, geodetic data alone, are not able to precisely constrain the thickness of the causative source. However, both interpretations are compatible with the observed ground deformation, gravity variations, and geochemical variations.

Concerning the source of the hydrothermal fluids, the most likely mechanism is the degassing of the magma batch which likely intruded at depth in the northwestern sector of the island. A similar mechanism is possibly related to the recent seismological and geochemical anomalies observed in Tenerife (D'Auria et al., 2019;

Padrón et al., 2021; Amonte et al., 2021). This magmatic injection episode did not show up in the ground deformation pattern, possibly because of the depth of the intrusion (>5 km) and the limited amount of magma involved. We note that eruptions occurring along the NW dorsal of Tenerife have generally a Strombolian character and are fed by basaltic magmas. This contrasts with the central Teide-Las Cañadas complex, where phonolitic eruptions with both effusive and explosive typologies occurred in the past. This was explained by Koulakov et al. (2023) by considering the difference in the crustal structure beneath these two areas. In the former, the rigid crust does not allow a long-term residence of primitive basaltic magmas, which quickly reach the surface through a network of dikes. In the latter, the presence of a ductile regime allows the stationing and the differentiation of magmas toward phonolitic composition. In this context, we postulate that the 2004–2005 unrest represents a "failed" eruption along the NW dorsal in Tenerife.

Our work highlights two relevant points from the volcano monitoring point of view. First, the most likely precursor of an eruption in the NE dorsal of Tenerife is deep seismicity related to the magmatic intrusion process. This is similar to what was observed during the 2021 Tajogaite eruption on the island of La Palma (D'Auria et al., 2022). Second, the ground deformation pattern should be interpreted carefully. We have shown how it can be related to a hydrothermal causative source instead of a magmatic intrusion.

Data availability statement

Publicly available datasets were analyzed in this study. This data can be found here: https://earth.esa.int/eogateway/missions/envisat/data.

Author contributions

MP: Conceptualization, Data curation, Formal Analysis, Investigation, Methodology, Visualization, Writing–original draft, Writing–review and editing. LD'A: Conceptualization, Data curation, Investigation, Methodology, Software, Writing–review and editing. SP: Data curation, Investigation, Writing–review and editing. PT: Conceptualization, Data curation, Investigation, Supervision, Writing–review and editing. AB: Investigation, Supervision, Writing–review and editing. AV: Investigation, Writing–review and editing. NP: Conceptualization, Writing–review and editing. RC: Conceptualization, Data curation, Investigation, Methodology, Software, Supervision, Writing–review and editing.

Funding

The author(s) declare that financial support was received for the research, authorship, and/or publication of this article. This work was supported by the projects VOLRISKMAC II (MAC2/3.5b/328), co-financed by the Interreg-MAC EU program and TFvolcano, financed by the Instituto Tecnológico y de Energías Renovables (ITER).

Conflict of interest

The authors declare that the research was conducted in the absence of any commercial or financial relationships that could be construed as a potential conflict of interest.

The handling editor PC declared a past co-authorship with the author LD.

Publisher's note

All claims expressed in this article are solely those of the authors and do not necessarily represent those of their affiliated organizations, or those of the publisher, the editors and the reviewers. Any product that may be evaluated in this article, or claim that may be made by its manufacturer, is not guaranteed or endorsed by the publisher.

References

Acernese, F., Amico, P., Arnaud, N., Babusci, D., Barillé, R., Barone, F., et al. (2004). Properties of seismic noise at the Virgo site. *Class. Quantum Gravity* 21 (5), S433–S440. doi:10.1088/0264-9381/21/5/008

Almendros, J., Ibáñez, J. M., Carmona, E., and Zandomeneghi, D. (2007). Array analyses of volcanic earthquakes and tremor recorded at Las Cañadas caldera (Tenerife Island, Spain) during the 2004 seismic activation of Teide volcano. *J. Volcanol. Geotherm. Res.* 160 (3-4), 285–299. doi:10.1016/j.jvolgeores.2006.10.002

Amonte, C., Asensio-Ramos, M., Melián, G. V., Pérez, N. M., Padrón, E., Hernández, P. A., et al. (2021). Hydrogeochemical temporal variations related to changes of seismic activity at Tenerife, Canary Islands. *Bull. Volcanol.* 83 (4), 24. doi:10.1007/s00445-021-01445-4

Barrera Morate, J. L., and García Moral, R. (2011). *Mapa Geológico de Canarias*. Santa Cruz de Tenerife: GRAFCAN.

Bottiglieri, M., Falanga, M., Tammaro, U., Obrizzo, F., De Martino, P., Godano, C., et al. (2007). Independent component analysis as a tool for ground deformation analysis. *Geophys. J. Int.* 168 (3), 1305–1310. doi:10.1111/j.1365-246x.2006.03264.x

Carracedo, J. C., Badiola, E. R., Guillou, H., Paterne, M., Scaillet, S., Torrado, F. P., et al. (2007). Eruptive and structural history of Teide volcano and rift zones of Tenerife, canary islands. *Geol. Soc. Am. Bull.* 119 (9-10), 1027–1051. doi:10.1130/b26087.1

Comon, P. (1994). Independent component analysis, a new concept? *Signal Process* 36, 287–314. doi:10.1016/0165-1684(94)90029-9

D'Auria, L., Barrancos, J., Padilla, G. D., Pérez, N. M., Hernández, P. A., Melián, G., et al. (2019). The 2016 Tenerife (Canary Islands) long-period seismic swarm. *J. Geophys. Res. Solid Earth* 124 (8), 8739–8752. doi:10.1029/2019jb017871

D'Auria, L., Koulakov, I., Prudencio, J., Cabrera-Pérez, I., Ibáñez, J. M., Barrancos, J., et al. (2022). Rapid magma ascent beneath La Palma revealed by seismic tomography. *Sci. Rep.* 12 (1), 17654. doi:10.1038/s41598-022-21818-9

De Barros, L., Martini, F., Bean, C. J., Garcia-Yeguas, A., and Ibáñez, J. (2012). Imaging magma storage below Teide volcano (Tenerife) using scattered seismic wavefields. *Geophys. J. Int.* 191 (2), 695–706. doi:10.1111/j.1365-246x.2012.05637.x

De Luca, C., Cuccu, R., Elefante, S., Zinno, I., Manunta, M., Casola, V., et al. (2015). An on-demand web tool for the unsupervised retrieval of Earth's surface deformation from sar data: the p-sbas service within the esa g-pod environment. *Remote Sens.* 7, 15630–15650. doi:10.3390/rs71115630

De Luca, C., Valerio, E., Giudicepietro, F., Macedonio, G., Casu, F., and Lanari, R. (2022). Pre-and co-eruptive analysis of the September 2021 eruption at Cumbre Vieja volcano (La Palma, Canary Islands) through DInSAR measurements

and analytical modeling. *Geophys. Res. Lett.* 49 (7), e2021GL097293. doi:10.1029/2021gl097293

Domínguez-Cerdeña, I., del Fresno, C., and Rivera, L. (2011). New insight on the increasing seismicity during Tenerife's 2004 volcanic reactivation. *J. Volcanol. Geotherm. Res.* 206 (1-2), 15–29. doi:10.1016/j.jvolgeores.2011.06.005

Ebmeier, S. (2016). Application of independent component analysis to multitemporal InSAR data with volcanic case studies. *J. Geophys.Res. Solid Earth* 121, 8970–8986. doi:10.1002/2016jb013765

Fernández, J., Tizzani, P., Manzo, M., Borgia, A., González, P. J., Martí, J., et al. (2009). Gravity-driven deformation of Tenerife measured by InSAR time series analysis. *Geophys. Res. Lett.* 36 (4). doi:10.1029/2008gl036920

García, A., Ortiz, R., Marrero, J. M., S´ nchez, N., Vila, J., Correig, A. M., et al. (2006). Monitoring the reawakening of canary islands' Teide volcano. *Eos, Trans. Am. Geophys. Union* 87 (6), 61–65. doi:10.1029/2006eo060001

Gottsmann, J., Camacho, A. G., Martí, J., Wooller, L., Fernández, J., Garcia, A., et al. (2008). Shallow structure beneath the Central Volcanic Complex of Tenerife from new gravity data: implications for its evolution and recent reactivation. *Phys. Earth Planet. Interiors* 168 (3-4), 212–230. doi:10.1016/j.pepi.2008.06.020

Gottsmann, J., Wooller, L., Martí, J., Fernández, J., Camacho, A. G., González, P. J., et al. (2006). New evidence for the reawakening of Teide volcano. *Geophys. Res. Lett.* 33 (20). doi:10.1029/2006gl027523

Hyvärinen, A., and Oja, E. (2000). Independent component analysis: algorithms and applications. *Neural Netw.* 13, 411–430. doi:10.1016/s0893-6080(00)00026-5

Koulakov, I., D'Auria, L., Prudencio, J., Cabrera-Pérez, I., Barrancos, J., Padilla, G. D., et al. (2023). Local earthquake seismic tomography reveals the link between crustal structure and volcanism in Tenerife (Canary Islands). *J. Geophys. Res. Solid Earth* 128 (3), e2022JB025798. doi:10.1029/2022jb025798

Márquez, A., López, I., Herrera, R., Martín-González, F., Izquierdo, T., and Carreno, F. (2008). Spreading and potential instability of Teide volcano, Tenerife, canary islands. *Geophys. Res. Lett.* 35 (5). doi:10.1029/2007gl032625

Martí, J., Ortiz, R., Gottsmann, J., Garcia, A., and De La Cruz-Reyna, S. (2009). Characterising unrest during the reawakening of the central volcanic complex on Tenerife, Canary Islands, 2004–2005, and implications for assessing hazards and risk mitigation. *J. Volcanol. Geotherm. Res.* 182 (1-2), 23–33. doi:10.1016/j.jvolgeores.2009.01.028

Melián, G., Tassi, F., Pérez, N., Hernández, P., Sortino, F., Vaselli, O., et al. (2012). A magmatic source for fumaroles and diffuse degassing from the summit crater of Teide Volcano (Tenerife, Canary Islands): a geochemical evidence for the 2004–2005 seismic–volcanic crisis. *Bull. Volcanol.* 74, 1465–1483. doi:10.1007/s00445-012-0613-1

Nelder, J. A., and Mead, R. (1965). A simplex method for function minimization. *Comput. J.* 7, 308–313. doi:10.1093/comjnl/7.4.308

Padrón, E., Pérez, N. M., Hernández, P. A., Melián, G., Asensio-Ramos, M., D'Auria, L., et al. (2021). Changes in diffuse degassing from the summit crater of Teide volcano (Tenerife, Canary Islands) prior to the 2016 Tenerife long-period seismic swarm. *J. Geophys. Res. Solid Earth* 126 (3), e2020JB020318. doi:10.1029/2020jb020318

Pepe, A., Manzo, M., Casu, F., Solaro, G., Tizzani, P., Zeni, G., et al. (2008). Surface deformation of active volcanic areas retrieved with the SBAS-DInSAR technique: an overview. *Ann. Geophys.* 51, 247–263.

Pepe, S., D'Auria, L., Castaldo, R., Casu, F., De Luca, C., De Novellis, V., et al. (2018). The use of massive deformation datasets for the analysis of spatial and temporal evolution of Mauna Loa volcano (hawai'i). *Remote Sens.* 10 (6), 968. doi:10.3390/rs10060968

Pérez, N. M., Hernández, P. A., Padrón, E., Melián, G., Nolasco, D., Barrancos, J., et al. (2013). An increasing trend of diffuse CO2 emission from Teide volcano (Tenerife, Canary Islands): geochemical evidence of magma degassing episodes. *J. Geol. Soc.* 170 (4), 585–592. doi:10.1144/jgs2012-125

Przeor, M., D'Auria, L., Pepe, S., Tizzani, P., and Cabrera-Pérez, I. (2022). Elastic interaction between Mauna Loa and Kīlauea evidenced by independent component analysis. *Sci. Rep.* 12 (1), 19863. doi:10.1038/s41598-022-24308-0

Tárraga, M., Carniel, R., Ortiz, R., Marrero, J. M., and García, A. (2006). On the predictability of volcano-tectonic events by low frequency seismic noise analysis at Teide-Pico Viejo volcanic complex, Canary Islands. *Nat. Hazards Earth Syst. Sci.* 6 (3), 365–376. doi:10.5194/nhess-6-365-2006

Tizzani, P., Berardino, P., Casu, F., Euillades, P., Manzo, M., Ricciardi, G. P., et al. (2007). Surface deformation of long valley caldera and mono basin, California, investigated with the SBAS-InSAR approach. *Remote Sens. Environ.* 108 (3), 277–289. doi:10.1016/j.rse.2006.11.015

Weber, K., Fischer, C., Van Haren, G., Bothe, K., Pisirtsidis, S., Laue, M., et al. (2006). "Ground-based remote sensing of gas emissions from Teide volcano (Tenerife, Canary Islands, Spain): first results," in *Remote sensing of clouds and the atmosphere XI* (Stockholm, Sweden: SPIE), 6362, 384–393. doi:10.1117/12.714411